

Bisphenol-A exposure alters liver, kidney, and pancreatic Klotho expression by HSP60-activated mTOR/autophagy pathway in male albino rats

Ahmed A. Morsi^{1,*}, Ezat A. Mersal^{2,3}, Ahmed Othman Alsabih⁴, Shaimaa Alakabawy⁵, Riham G. Elfawal^{5,6}, Eman M. Sakr^{3,7}, Eman Mohamed Faruk^{8,9}, Mohammed Abu-Rashed¹⁰, Fatimah Alhaddad¹⁰, Zahra Alkhawajah¹⁰, Abdulrahman Hasari¹⁰, Khalid Elfaki Ibrahim¹¹, Ahmed M. Abdelmoneim¹²

¹ Department of Histology and Cell Biology, Faculty of Medicine, Fayoum University, Fayoum, Egypt

² Biochemistry Department, Faculty of Science, Assiut University, Assiut, Egypt

³ Department of Basic Medical Sciences, Vision Colleges, Riyadh, Saudi Arabia

⁴ Department of Physiology, College of Medicine, King Saud University, Riyadh, Saudi Arabia

⁵ Department of Clinical Sciences, Vision Colleges, Riyadh, Saudi Arabia

⁶ Clinical Pathology Department, Faculty of Medicine, Alexandria University, Alexandria, Egypt

⁷ National Institute of Oceanography and Fisheries (NIOF), Egypt

⁸ Anatomy Department, College of Medicine, Umm Al-Qura University, Makkah, Saudi Arabia

⁹ Department of Histology and Cytology, Faculty of Medicine, Benha University, Benha, Egypt

¹⁰ Medical students, Vision Colleges, Riyadh, Saudi Arabia

¹¹ Department of Zoology, College of Science, King Saud University, P.O. Box 2455, Riyadh 11451, Saudi Arabia

¹² Department of Physiology, Faculty of Medicine, Fayoum University, Fayoum, Egypt

ARTICLE INFO

Original paper

Article history:

Received: May 05, 2023

Accepted: July 02, 2023

Published: July 31, 2023

Keywords:

Cell stress and senescence, endocrine disruptors, environmental pollution, Klotho and HSP60 immunohistochemistry, rat gene study of *ULK1*

ABSTRACT

The effect of bisphenol-A (BPA) on Klotho protein (aging-suppressing protein) expression in different body organs has not been sufficiently addressed by literature studies. The study investigated the impact of BPA on Klotho expression in multiple organs including the liver, kidney, and pancreas and suggested the involved molecular pathways. Twenty-seven male Wistar albino rats were divided into 3 equal groups: control, low-dose BPA (4.5 µg/L), and high-dose BPA (8 µg/L) groups in drinking water for 45 consecutive days. Liver, kidney, and pancreatic specimens were prepared for a gene study of *Klotho*, *HSP60*, *mTOR*, and *ULK1* mRNA expressions. Also, the tissue specimens were measured for malondialdehyde (MDA), superoxide dismutase (SOD), and nitric oxide (NO) levels. Paraffin-embedded sections were also prepared and subjected to Hematoxylin and Eosin (H&E) staining and immunohistochemical detection of Klotho and HSP60. The results revealed an alteration in the MDA, SOD, NO tissue levels, disturbed gene expression profile, and apoptotic changes in the histological findings of the examined organs which were obvious ($p < 0.05$) in the high-dose group. The anti-aging *Klotho* gene/protein expression was reduced ($p < 0.05$) more in the high-dose BPA group than in the low dose. In contrast, *HSP60* gene/protein expression was significantly increased ($p < 0.05$) more in the high dose. The increased mTOR gene expression was strongly correlated ($p < 0.05$) with the decreased autophagy related gene *ULK1*. It was concluded that BPA exposure contributed to cell stress and markedly reduced Klotho protein expression in liver, kidney, and pancreatic tissues, possibly by modulation of the HSP60-activated mTOR/autophagy signaling.

Doi: <http://dx.doi.org/10.14715/cmb/2023.69.7.18>

Copyright: © 2023 by the C.M.B. Association. All rights reserved. 

Introduction

Bisphenol A (BPA) is a universal toxicant that is present in the surrounding environment. It is introduced in the industrial manufacture of epoxy resin and polycarbonate to promote the transparency, durability, and strength of some end products such as baby bottles, compact discs, medical and electronic devices (1).

Klotho is a single transmembrane protein including α , β , and γ Klotho members. Alpha Klotho isoform is the main member while, β and γ isoforms have relative structural similarity with α -klotho (hereafter referred to as Klotho) (2). Klotho is typically expressed in the kidneys. Extrarenal locations include choroid plexus, pituitary, parathyroid glands, heart, and pancreas, with low or even absent levels

in other tissues. Despite its low levels or absence in these tissues, it is still essential to preserve their normal function (3,4). Klotho is described as a biomarker for aging and longevity. Klotho knockout mice models were associated with disease, meanwhile, klotho overexpression was correlated with improved health and life span expansion (5).

Autophagy is a highly selective catabolic pathway aiming at the clearance of defective cellular components, such as dead organelles and accumulated mis/unfolded proteins. Therefore, loss of basal functional autophagy leads to the accumulation of damaged proteins, proteotoxicity, and cellular senescence (6). The machinery of autophagy is regulated by several autophagy-related genes (ATG). For example, unc-51-like autophagy activating kinase (ULK)1, synonym to ATG1, is involved in the ini-

* Corresponding author. Email: aaa21@fayoum.edu.eg

tiation of autophagy (7).

Heat Shock Proteins (HSPs) are intracellular molecules expressed as a reaction to various stressors related to aging, not just thermal stress. According to their molecular weight, HSPs are a big family with different HSPs members such as HSP40, HSP60, and HSP70 (8,9). Once a cell is exposed to a low dose, non-toxic environmental stressor (e.g. radiation, infection, heavy metal, and chemicals) followed by a molecular and or physiological deficit, HSPs are further upregulated to repair such damage and provide an anti-aging adaptive response by maintaining cell integrity and functionality, a state called “hormesis” effect (10,11). HSP60 is a 60-kilodalton mitochondrial chaperone whose folding activity keep the mitochondria safe against proteotoxicity induced by the unfolded denatured proteins that arise under different types of stressors (12).

The mechanistic target of the rapamycin (mTOR) pathway is a protein kinase that orchestrates the balance between cell growth and cell degradation-mediated autophagy by sensing different environmental and intracellular signals such as dietary status, growth factors, and stress signals (13). Several studies stated a direct link between mTOR signaling and aging biomarkers being entangled in some of the aging hallmarks/attributes. Activated mTOR signaling represses autophagy by phosphorylating two indispensable autophagy starter proteins, ULK1 and ATG13 so, mTOR pathway inactivation induces autophagy machinery (14,15). mTOR/HSP60 interaction was reported in the literature (16), in which the activation of the latter was associated with mTOR enhancement.

The current study investigated whether environmentally relevant dose levels of BPA affect Klotho expression in the major body organs. The study hypothesized an inhibitory effect of BPA on the expression of the aging-suppressing protein Klotho in the liver, kidney, and pancreas in male albino rats. Therefore, the research evaluated the gene/protein expression of Klotho and assumed mTOR/autophagy modulation via HSP60 activation.

Materials and Methods

Chemicals

Bisphenol-A, (Catalog #: 239658, BPA, $\geq 99\%$ purity), was purchased from Sigma-Aldrich (Saint Louis, MO, USA).

Ethical statement

The proposal of the study was granted ethical approval by the Institutional Review Board (IRB), College of Medicine, King Saud University, Saudi Arabia (IRB #: KSU-SE-20-37). All experimental procedures adhered to The U.S. Public Health Service Policy on Humane Care and Use of Laboratory Animals, available from the Office of Laboratory Animal Welfare (<https://olaw.nih.gov/>). All experimental manipulations were taken into consideration to humanely manage the animals to diminish animal struggle, pain, and distress.

Animals and experimental groups

Twenty-seven Wistar male albino rats (4-6-week-old, 200 \pm 20 g bodyweight) were used in the current experiment. It was conducted in the Experimental Surgery and Animal Laboratory (ESAL) of the College of Medicine, King Saud University, Saudi Arabia. The animals were

locally bred and purchased from the ESAL's colony breeding unit. The rats were group housed (25 \pm 1 °C, 12-hour light/dark cycles) and were given *ad libitum* access to food and water. Water supply was delivered in glass bottles, meanwhile, the animals were housed in polypropylene (BPA free)-made cages. For laboratory adaptation, the animals were left for one week before the beginning of the experiment. The rats were randomly divided into 3 equal groups, 9 rats each:

- Control group: The animals received distilled water containing equal volumes of ethanol 30 % (corresponding vehicle for BPA) for 45 days.
- Low-dose BPA group: The animals received Bisphenol-A in drinking water (4.5 μ g/L) for 45 days.
- High-dose BPA group: The animals received Bisphenol-A in drinking water (8 μ g/L) for 45 days.

BPA was dissolved in 30% ethanol according to Moon et al. (17). Dilution was done by adding distilled water to reach a final concentration of 4.5 and 8 μ g/L. The selection of low-BPA dose was based on the average of the environmental levels reported by the authors' research team (18) to mimic the relevant human exposure in the low-dose group. The high-dose BPA was equivalent to double the tolerable daily intake (TDI) that was set at 4 μ g/kg/d as declared by European Food Safety Authority (19).

Tissue sample collection

At the end of the study, the animals were anaesthetized and sacrificed by cervical dislocation. The abdomens were explored, and the livers, kidneys, and pancreata were removed and washed in cool saline. Each organ was divided into 2 portions. One portion was frozen at -80°C for later measurement of tissue malondialdehyde (MDA), superoxide dismutase (SOD), and nitric oxide (NO), and gene study of *Klotho*, *HSP60*, *mTOR*, and *ULK1*. The other portion was fixed in formol saline for paraffin processing and histological study.

Tissue homogenate preparation for inflammatory and oxidative assays

The frozen part of each corresponding organ was homogenized separately in 10 ml cold potassium phosphate buffer solution (50 mM, pH 7.5) at 4 °C using an Ultra-Turrax tissue homogenizer (IKA, Germany). Centrifugation (3000 rpm) was done for 15 min at 4 °C and the resultant supernatant was collected for estimation of the tissue levels of MDA, SOD, and NO (Abcam, Cambridge, UK, catalog #: ab233471, ab65354, ab65328 respectively). MDA measurements were expressed in nmol/mg protein using Thiobarbituric acid reactive substances (TBARS) assay (20). SOD (U/mg protein) and NO levels (nmol/mg protein) were measured according to sun et al. (21) and Montgomery and Dymock (22) respectively. The manufacturer's recommendations were followed during the laboratory assay of each.

RT-PCR analysis of *Klotho*, *HSP60*, *mTOR*, and *ULK1* gene expression

The collected liver, kidney, and pancreas samples were thoroughly homogenized and prepared for the gene study. Initially, the total RNA was isolated and extracted from the three samples using RNeasy Mini Kit (Qiagen, USA, Cat No./ID: 74104). The concentration of the total RNA was measured by spectrophotometry (JENWAY, USA) at

Table 1. Oligonucleotide primers sequences used in the q-PCR analysis for the studied genes.

Targeted gene	Primers sequences (Forward and Reverse primers)
<i>Klotho</i>	Forward:5'- GATAGAGAAAAATGGCTTCCCTCC-3' Reverse:5'- GGTCGGTAAACTGAGACAGAGTGG-3'
<i>HPS60</i>	Forward:5'- AAATCCGGAGAGGTGTGATG-3' Reverse:5'- CTTCAGGGGTTGTACAGGT-3'
<i>mTOR</i>	Forward:5'- AGAGGACCAGCAGCACAAGCAG -3' Reverse:5'- TGGTGGCAGTGGTGGTGGCATTG -3'
<i>ULK1</i>	Forward:5'- CCCCAACCTTTCGGACTT -3' Reverse:5' - CCAACAGGGTCAGCAAACCTC 3'
<i>GAPDH</i>	Forward:5'- AGTGCCAGCCTCGTCTCATA-3' Reverse:5'- ACCAGCTTCCCATTCTCAGC-3'

260/280 nm following the manufacturer's protocol. cDNA was synthesized for all gene markers from the corresponding mRNA using an iScript™ kit (Bio-Rad Hercules, CA) according to the manufacturer's recommendation. Glyceraldehyde 3-phosphate dehydrogenase (*GAPDH*) was used as a housekeeping gene for comparison/normalization of gene expression data. StepOnePlus™ real-time PCR system using software version 3.1 (Applied Biosystems, USA) in 7500 Fast thermal cycler system (2 µl of first strand DNA and 1 µl of 18 µM primer mixture in 20 µl total volume) was used to evaluate the reaction and quantify the samples. The primer sequences used in the qRT-PCR measurements of *Klotho*, *HPS60*, *mTORC1*, *ULK1*, and *GAPDH* were recorded in Table 1.

Histological and Immunohistochemical procedures

The specimens assigned for histological examination were fixed in formol saline (10%) for two days, then processed for paraffin sections. For each organ, five-micrometer sections were cut and stained with hematoxylin and eosin (23). The immunohistochemical technique was used for the identification of aging biomarkers; *Klotho* and HSP60 (24). For *Klotho* and HSP60, the primary antibodies were rabbit polyclonal and monoclonal antibodies, respectively (Abcam, Cambridge, UK, Catalog #: ab203576, ab190828). The kidney, liver, and pancreatic sections were boiled in citrate buffer (at pH 6 and 95° C). Next, the primary antibody was diluted (1:400 for *Klotho* and 1:2000 for HSP60) in PBS and was incubated with the sections for 60 min. The secondary kits used for the completion of the immunostaining were rabbit-specific HRP/DAB detection kits (Catalog #: ab64261, Abcam, Cambridge, UK). The chromogen and nuclear counterstaining were 3,3-diaminobenzidine (DAB) and hematoxylin respectively. The immunopositivity appeared as brownish cytoplasmic immunostaining. The positive control, for *Klotho*, was the cytoplasmic reaction of rat kidney tissues. The positive control for HSP60 was rat liver. The negative control was prepared by skipping the step of the primary antibody (Fig 1). The slides were visualized and photographed using an Olympus DP72 camera installed on an Olympus BX51 microscope (Olympus Corporation, Tokyo, Japan), connected to a computer system provided with cellSens 1.4.1 software.

Histomorphometric study

The image photomicrography and analysis were done in the Department of Anatomy, College of Medicine, King Saud University, Saudi Arabia. For image analysis, the

measurements were done blindly by a pathologist who was unfamiliar with the study groups. At 20x magnification, all immunostained slides were scanned by a slide scanner (Leica Aperio CS2, Leica Biosystems Imaging, Inc., Germany). The computer system was provided with Aperio ImageScope software v12.4.3 (Leica Biosystems Imaging, Inc., Germany). Next, all scanned slides were subjected to image analysis using the software's color deconvolution algorithm to measure the area percent and the optical density. Ten rectangular fixed areas of interest (1.920 mm²) in each section per group were randomly selected. For *Klotho*, the area percent was measured in the kidney and pancreas, meanwhile the optical density in the liver. The HSP60 immunoreaction was quantified by measuring the optical density in the three organs. Data were then exported, and statistical analysis was performed.

Statistical analysis

All data generated were subjected to statistical analysis using One-way Analysis of Variance (ANOVA) to detect significance. Comparison between the animal groups was done using post hoc Tukey's test. Also, a correlation analysis using Pearson's correlation coefficient was done to evaluate whether a relationship exists between *mTOR* and *ULK1* mRNA expressions. An initial check of even dis-

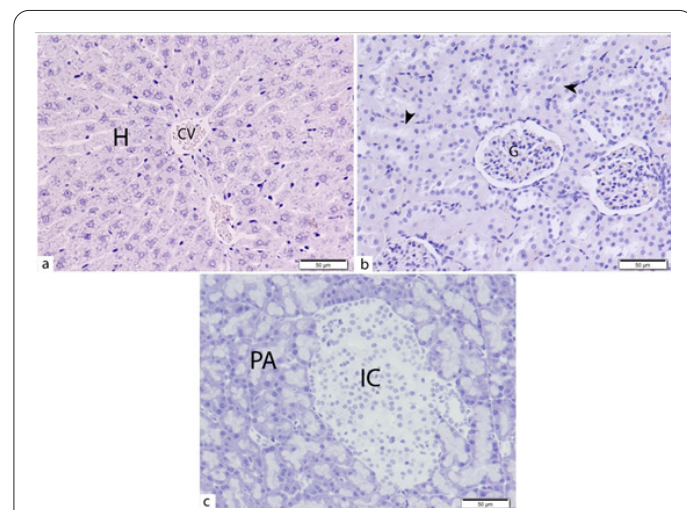


Figure 1. Immune-light photomicrographs representative of the negative control sections of the liver (a), kidney (b), and pancreas (c) of the study groups. Panel (a) shows unlabeled hepatocytes (H) around the central vein (CV). Panel (b) shows unlabeled (negatively reacted) renal tubules (arrowheads) and renal glomeruli (G). Panel (c) shows immune-negative pancreatic islets (IC) and pancreatic acini (PA). Scale bar: 50 µm.

tribution was carried out before the analysis using Shapiro's test. GraphPad Prism (GraphPad Software, Version 8 for Windows, San Diego, California, USA) was used to analyze all research data. Data were conveyed as mean ± standard deviation and statistical significance was considered at $p < 0.05$. For sample size determination, G*power software version 3.0.10 (25) was used. The software was set at an a priori type of power analysis, alpha level 5%, power 80 and a desired effect size 0.70; predetermined according to our own scientific knowledge, experience in the field area, and searching the literature for parallel finding of similar studies. Hence, nine rats per group were statistically adequate.

Results

Effect of BPA exposure on the MDA, SOD, and NO levels in tissue homogenates

The tissue concentrations of MDA, SOD, and NO were measured in the liver, kidney, and pancreas (Fig 2). Both BPA groups showed a substantial rise ($p < 0.05$) in MDA when compared to each control organ, however, the increase in NO was only significant ($p < 0.05$) in the high-dose group. SOD tissue levels were markedly decreased ($p < 0.05$) in the examined organs of both BPA groups. When the two BPA groups were compared, the NO and MDA were extreme ($p < 0.05$) in the high-dose group, meanwhile SOD was reduced ($p < 0.05$).

Effect of BPA on *Klotho*, *HSP60*, *mTOR*, and *ULK1* genes expression

When compared to control values, *Klotho* expression was significantly down-regulated ($p < 0.05$) in the kidneys, pancreas, and livers of both low and high-dose-BPA groups, although it was non-significant only in the liver of the low-dose group. *HSP60* mRNA expression was significantly upregulated ($p < 0.05$) in the three organs of both BPA groups, although the increase was non-significant only in the kidney of the low-dose group, in comparison to the control. Both BPA doses significantly increased ($p < 0.05$) *mTOR* mRNA levels in the three organs, in relation to the control group. On the opposite, the autophagy gene; *ULK1* expression was significantly down-regulated ($p < 0.05$), in the three organs when compared to their control (Fig 3). Correlation analysis showed a strong negative correlation ($r = -0.641$) with *mTOR*.

Effect of BPA exposure on the histological structure of the liver, kidney, and pancreas

The H&E-stained control liver sections exhibited normal hepatic architecture. The hepatocytes showed acidophilic granular cytoplasm with vesicular nuclei and were

organized in pericentrally radiated plates. The hepatic blood sinusoids were lined by endothelial cells and Kupfer cells. The portal area showed the portal triad (Fig 4a, b). The low-dose BPA group showed approximately normal hepatic microstructure except for a few apoptotic hepatocytes

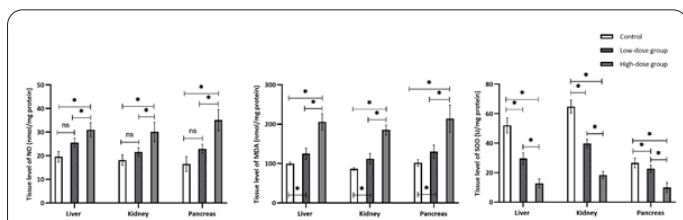


Figure 2. Changes in the tissue levels of MDA, SOD, and NO in the liver, kidney, and pancreas after 2-dose-BPA exposure. * Significant difference at $p < 0.05$ using One-Way ANOVA post hoc Tukey's test. ns: non-significant.

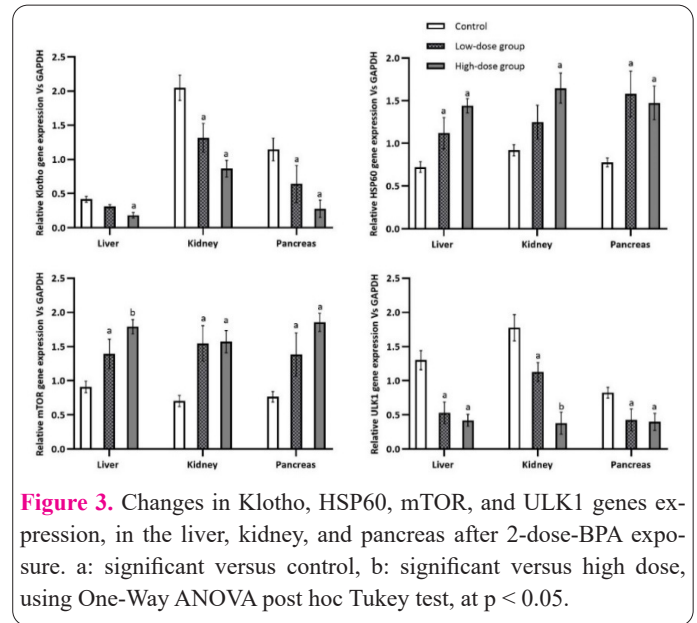


Figure 3. Changes in *Klotho*, *HSP60*, *mTOR*, and *ULK1* genes expression, in the liver, kidney, and pancreas after 2-dose-BPA exposure. a: significant versus control, b: significant versus high dose, using One-Way ANOVA post hoc Tukey test, at $p < 0.05$.

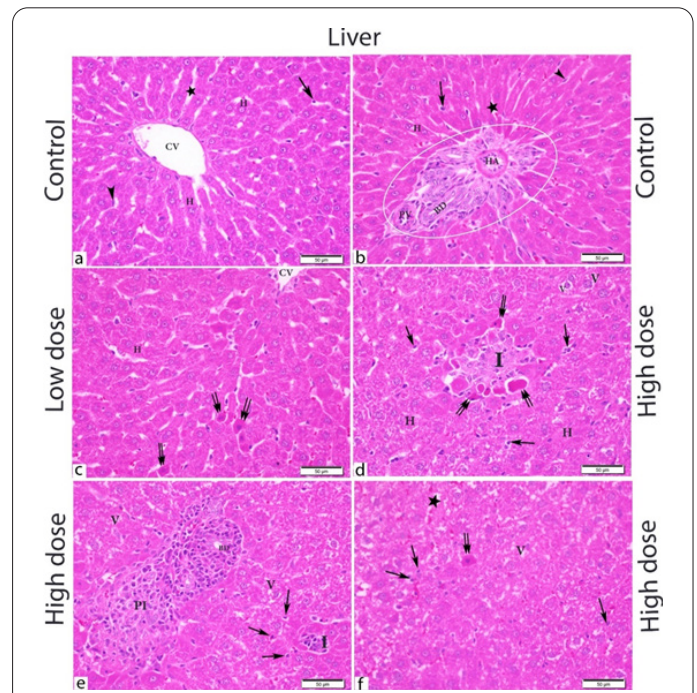


Figure 4. Effect of the two-dose-BPA exposure on the histological structure of the liver in the study groups. Control group (a, b) shows polyhedral hepatocytes (H) with acidophilic granular cytoplasm and vesicular nuclei. They are arranged in plates spreading from the central vein (CV) with intervening blood sinusoids (star) lined by Kupfer (arrow) and endothelial cells (arrowhead). The portal area (circle) shows branches of the portal triad (portal vein (PV), hepatic artery (HA), and bile duct (BD)). Low-dose BPA group (c) shows few scattered apoptotic hepatocytes (double arrows). High-dose BPA group (d-f) shows marked hepatic disorganization (H) with vacuolar changes (V). Mononuclear cellular infiltrations have either a parenchymal distribution (I) or located periportal (PI). Numerous apoptotic hepatocytes (double arrows) are randomly observed, and others are seen around the cellular infiltrates. Liver blood sinusoids (star) are congested and lined by hyperplastic and hypertrophic Kupfer cells (arrows). H & E-stained photomicrographs, scale bar: 50 μ m

cytes indicated by their darkly stained pyknotic nuclei and eosinophilic cytoplasm (Fig 4c). However, the high-dose group showed a disorganized hepatic array with vacuolar degenerative changes. Multiple foci of mononuclear cell infiltrates were seen replacing hepatocytes (Fig 3d) and others were infiltrating the portal area around the portal triad (Fig 4e). Numerous apoptotic hepatocytes were seen at the periphery of the cell infiltrates (Fig 4e), and others were seen scattered in the liver parenchyma (Fig 4f). The blood sinusoids were congested and were lined by notable hyperplastic and hypertrophied Kupffer cells (Fig 4f).

The control kidney sections displayed normal renal parenchyma. The renal corpuscles appeared with normal glomeruli, Bowman's capsules, and normal urinary spaces. The proximal convoluted tubules (PCT) appeared with a

narrow lumen and were lined by pyramidal cells with clear apical brush borders. The distal tubules (DCT) showed wide lumen and were lined by cubical cells (Fig 5a). The low-dose BPA group showed a disturbed apical brush border of the renal tubules (Fig 5b). However, the high-dose group showed frequent atrophic glomeruli, interstitial vascular congestion, tubular vacuolar changes with loss of the brush border, and extensive interstitial inflammatory cell infiltrates (Fig 5c, d).

The control pancreatic sections showed normal histological architecture of the pancreatic acini and islet cells. The islet cells appeared as vascularized masses of cells supported by reticular stroma all around. The exocrine pancreas showed normal acinar structure (Fig 5e). In the low-dose BPA group, the peripherally located pancreatic alpha cells showed apoptotic changes with clear halos all through. The central beta cells seemed normal (Fig 5f). The pancreatic islet cells in the high-dose group showed remarkable atrophy along with alpha/beta cell vacuolar and apoptotic changes (Fig 5g). Also, the pancreatic acini were extensively infiltrated by mononuclear inflammatory cells (Fig 5h).

Effect of BPA exposure on Klotho immunoexpression in liver, kidney, and pancreas

The anti-aging biomarker, Klotho showed constitutive cytoplasmic expression, in the control liver (Fig 6a, b), kidney (Fig 7a), and control pancreas (Fig 7d). Klotho expression showed pericentral and periportal preferences in the control liver and apical brush borders of the renal tubules in the control kidneys. In the low-dose BPA group, the liver sections showed a marked loss of the characteristic periportal and pericentral immunostaining (Fig 6c), and the kidney sections showed a moderate decrease in the tubular klotho expression (Fig 7b) meanwhile, the pancreatic sections showed a patchy distribution of the Klotho

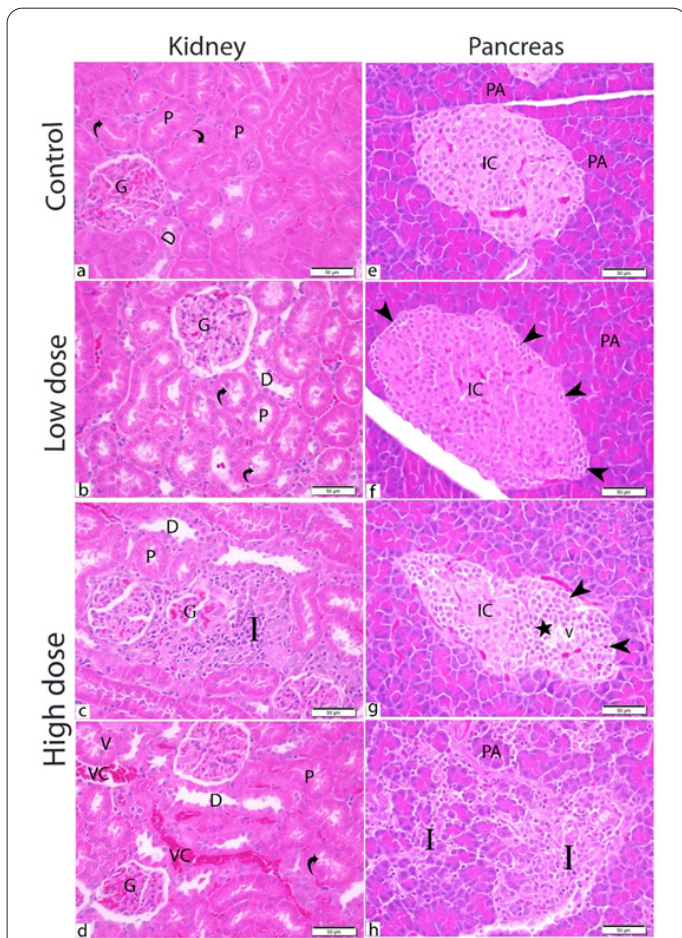


Figure 5. Effect of the two-dose-BPA exposure on the histological structure of the kidney and pancreas in the study groups. a-d: kidney sections. e-h: pancreatic sections. Control group (a) shows normal glomeruli (G). The PCT (P) shows a narrow lumen, lined by pyramidal cells with clear apical brush borders (curved arrows). The DCT (D) shows a wide lumen lined by cubical cells. Low-dose BPA group (b) shows a disturbed apical brush border (curved arrow) of the proximal tubules (P). High-dose BPA group (c, d) shows marked atrophy of the renal glomeruli (G), interstitial vascular congestion (VC), tubular vacuolar changes (V) with loss of the brush border (curved arrow), and interstitial inflammatory cell infiltrates (I). Control group (e) shows normal pancreatic acini (PA) and normal islet cells (IC). Low-dose BPA (f) shows apoptotic peripherally located alpha cells (arrowheads). High-dose BPA group (g, h) shows atrophic islet cells (IC) with apoptotic changes in both alphas (arrowheads) and centrally located beta cells (star) with vacuolar changes (V). An extensive mononuclear cellular infiltration (I) is observed in between the acini. H & E-stained photomicrographs, scale bar: 50 μ m.

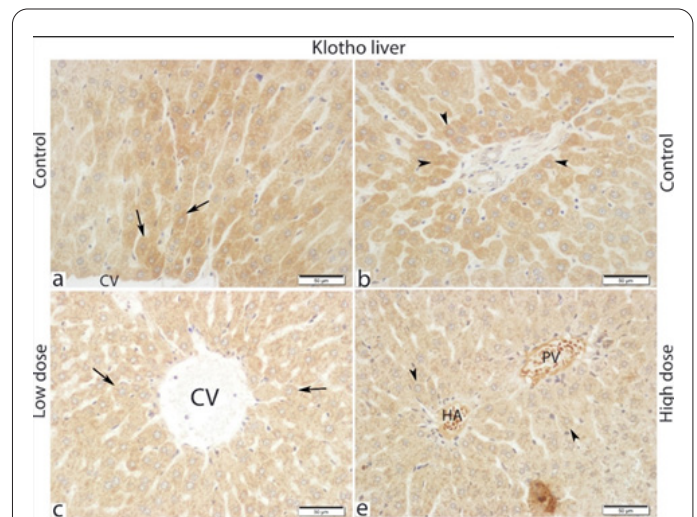


Figure 6. Effect of the two-dose-BPA exposure on the immunohistochemical expression of Klotho in the livers of the study groups. Control group (a, b) shows diffuse weak cytoplasmic klotho expression with marked hepatocytes expression (arrows) around the central vein (CV) and those (arrowheads) around the portal tract. Both low (c) and high dose (e)-exposed groups show loss of the characteristic pericentral (CV) and periportal klotho distribution. The portal tract is indicated by the presence of hepatic artery (HA) and portal vein (PV) branches. Anti-Klotho immune-light photomicrographs, scale bar: 50 μ m.

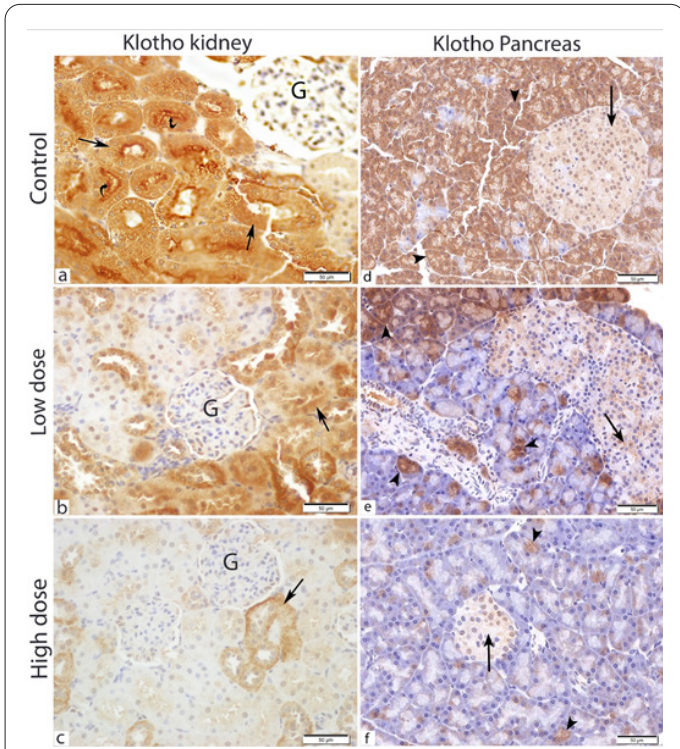


Figure 7. Effect of the two-dose-BPA exposure on the immunohistochemical expression of Klotho in the kidneys and pancreas of the study groups. a-c: kidney immunostaining. d-f: pancreas immunostaining. Control group (a) shows marked cytoplasmic klotho expression in the renal tubules (arrows) with prominent apical brush border immunopositivity (curved arrows). The renal glomeruli (G) are faintly reacted. Low-dose BPA group (b) shows a notable decrease in the renal tubular klotho expression (arrow) sparing renal glomeruli (G). High-dose group (c) shows diffuse faint klotho immunostaining and few renal tubules show weak reaction (arrow). Control group (d) shows diffuse cytoplasmic klotho immunopositivity in pancreatic acini (arrowheads) and faint islet cells (arrow) reaction was observed. Low-dose BPA group (e) shows scattered acinar (arrowheads) and islet cell (arrow) immunoreactions. High-dose group (f) shows a diffuse negative reaction. Very few acinar reactions are noticed (arrowheads) and islet cells (arrows) show negative reactivity. Anti-Klotho immune-light photomicrographs, scale bar: 50 μm .

immunoreaction (Fig 7e). In the high-dose group, a further decrease in klotho expression was noticed in the liver (Fig 6d), kidney (Fig 7c), and pancreatic sections (Fig 7f).

Effect of BPA exposure on HSP60 immunoreaction in liver, kidney, and pancreas

In the control sections, HSP60 showed very faint immunoreactivity in the liver (Fig 8a), very mild expression in the kidneys (Fig 8d), and negative pancreatic reaction (Fig 8g). In the low-dose BPA group, the liver sections showed diffuse intense hepatocyte HSP60 immunoreaction (fig 8b), the kidney sections showed a mild increase

in the HSP60 tubular immunostaining (Fig 8e) meanwhile, the pancreatic sections showed islet cell immunoreaction with obvious alpha cell immunopositivity (Fig 8h). In the high-dose group, the liver cells (Fig 8c), renal tubules (fig 8f), and pancreatic islets (Fig 8i) showed an increase in the HSP60 reaction intensity.

Effect of BPA on Klotho and HSP60 morphometric measurements in the examined organs

Klotho expression was morphometrically quantified by measurement of the mean optical density in the liver and calculating the mean area percent in the kidney and pancreas (Table 2). In comparison with the control groups, the low-dose group showed a statistically significant decrease ($p < 0.05$) in klotho expression in the three organs. There was a substantial decrease ($p < 0.05$) in the high-dose BPA group when compared to the low-dose group. HSP60 expression was measured by the determination of the mean optical density in the liver, kidney, and pancreas (Table 3). HSP60 protein was expressed ($p < 0.05$) in the three

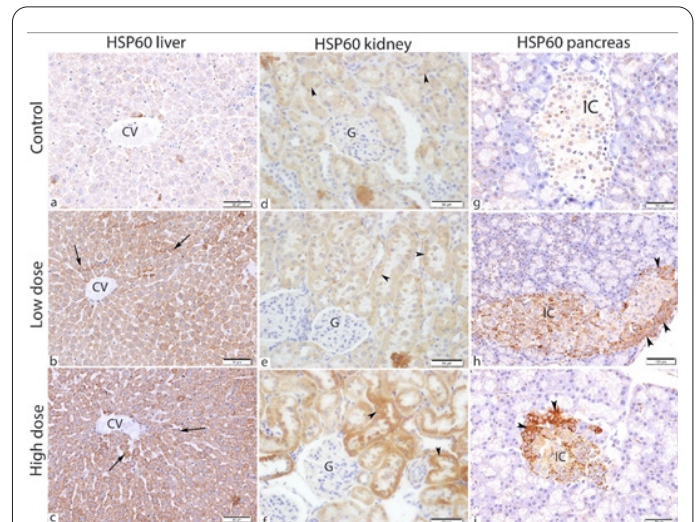


Figure 8. Effect of the two-dose-BPA exposure on the immunohistochemical expression of HSP60 in the liver, kidney, and pancreas of the study groups. a-c: liver immunostaining. d-f: kidney immunostaining. g-i: pancreas immunostaining. Control group (a) shows very faint immunoreaction. Low-dose BPA group (b) shows diffuse intense hepatocyte immunoreactivity (arrows). The reaction intensity increased in the high-dose group (c). Control group (d) shows faint renal tubules' immunopositivity (arrowheads) sparing renal glomeruli (G). The reaction intensity mildly increased in the low-dose group (e) and markedly expressed in the high-dose group (f). Control group (g) shows negative HSP60 immunoreactivity. Low-dose and high-dose groups (h, i respectively) show the islet cells (IC) with HSP60 positive immunoreaction mainly stains the peripherally located alpha cells (arrowheads) and are more marked in the high-dose group. Anti-HSP60 immune-light photomicrographs, scale bars. a-i: 50 μm ; h: 100 μm .

Table 2. Effect of the two-dose-BPA exposure on the morphometric measurements of Klotho immunoreaction in the liver, kidney, and pancreas.

Parameter/group	Control group	Low-dose BPA group	High-dose BPA group
Optical density in the liver	0.844±0.07	0.528±0.12 ^a	0.299±0.11 ^{ab}
Area percent in kidney (μm^2)	75.48±6.55	48.35±4.49 ^a	18.79±1.97 ^{ab}
Area percent in pancreas (μm^2)	67.48±3.12	57.26±5.19 ^a	11.56±1.37 ^{ab}

The records were presented as mean \pm SD, n= 9, using one-way ANOVA post hoc Tukey's test at $p < 0.05$. ^a significant versus control. ^b significant versus low-dose group.

Table 3. Effect of the two-dose-BPA exposure on the morphometric measurements of HSP60 immunoeexpression in the liver, kidney, and pancreas.

Parameter/group	Control group	Low-dose BPA group	High-dose BPA group
Optical density in the liver	0.281±0.14	0.497±0.13 ^a	0.834±0.07 ^{ab}
Optical density in kidney	0.32±0.17	0.48±0.14 ^a	0.63±0.11 ^{ab}
Optical density in pancreas	0.30±0.1	0.48±0.12 ^a	0.58±0.21 ^{ab}

The records were presented as mean ± SD, n= 9, using one-way ANOVA post hoc Tukey's test at p < 0.05. ^a significant versus control. ^b significant versus low-dose group.

organs of the low-dose BPA group when compared to the control group. The high-dose group showed a substantial increase ($p < 0.05$) when compared with the low-dose.

Discussion

The study's findings revealed a statistically significant reduction in the tissue expression of Klotho in the kidney, liver, and pancreas of BPA-exposed rats. The results suggested BPA as an environmental risk factor contributing to the aging process. This was proven by the molecular and immunohistochemical results of the anti-aging Klotho protein and cell stress marker HSP60, in addition to histological and biochemical methods. In the current experiment, the kidneys, liver, and pancreas were selected for investigation of the tissue expression of Klotho owing to their common affection for chronic diseases, regularly associated with aging e.g. diabetes mellitus, chronic liver, and kidney diseases (26). The male gender of rats was selected to abolish the protective estrogen effect on different organs, in female genders (27).

The pro-inflammatory and oxidative stress exerted by BPA in different literature studies (28,29) has paid the authors' attention to study its influence on the life span and cellular longevity. The current study investigated the effect of two BPA doses, low-dose (4.5 µg/L) and high-dose (8 µg/L) on the liver, kidney, and pancreatic tissues and showed a significant decrease of Klotho immunoeexpression, in the three organs when compared to the control group. The decrease was extreme in the high-dose rather than in the low-dose group.

Klotho is an anti-aging protein, constitutively expressed in many tissues mainly the kidneys and was reported to be protective against diseases via different mechanisms e.g. antioxidant, anti-inflammatory, anti-apoptotic, in addition to the regulation of phosphate/calcium metabolism (4). The current study reported Klotho gene/protein downregulation in BPA-exposed groups which might be related to an inflammatory cytokine effect. In harmony, the H & E findings disclosed mononuclear inflammatory cell infiltrates in the liver, kidney, and pancreas coupled with a significant rise in the tissue levels of nitric oxide and MDA, indicating a state of inflammation and oxidative stress after BPA exposure, in particular, high dose. The authors suggested a significant role for these cell infiltrates being the source of NO and MDA which were more significantly increased in the high-dose group, leading to further cell stress. The released mediators might induce Klotho downregulation in the three organs which was marked in the high dose. Such an explanation was consistent with Kim et al. (30) who found an upregulation of TNF-α and Klotho inhibition in radiation-induced senescent kidney cells. In the same context, Zou et al. (31) declared an interaction and a bidirectional relationship between Klotho and inflammation, meaning that inflammation may down-regulate Klotho ex-

pression (which was suggested herein), while Klotho can suppress inflammation. In mice with septic inflammation, Yan et al. (32) recorded Klotho downregulation-associated myocardial damage, which was reversed after exogenous Klotho supplementation.

Heat Shock Proteins (HSPs) are indicator molecules of increased cell stress. An individual's life span is determined by his/her resistance to both internal and external stressors. The HSPs decline, over time, with aging may be related to the failure of the heat shock transcription factor (HSF1) to combine HSP genes (9,33). This resistance is facilitated by HSP gene/protein expression during aging promoting proteostasis and expanding the life span. An unbalanced heat shock response (HSR) system can lead to the accumulation of aggregated unfolded damaged proteins in aged organisms and hence the occurrence of disease. Therefore, the overexpression of HSPs is an indicator of a within-limits trial of the body to combat aging, and delay the onset and or progression of diseases (11).

The gene study revealed that HSP60 expression was significantly elevated in both dose groups when compared to the control. The high-dose group showed a significant increase in comparison with the low-dose group. In accordance, the mean optical density of HSP60 immunostaining showed a significant rise in the liver, kidney, and pancreatic sections, which was markedly increased in the high-dose group. Therefore, such increased HSP60 expression could indicate cellular stress occurring in the liver, kidney, and pancreas and might refer to a balanced stress cell response mediated by HSP, and the loss of such balance might contribute to chronic inflammation and progression of aging as mentioned by Gomez (9). In agreement, Sun et al. (34) reported uremia-mediated stress-induced renal upregulation of HSP60 in rats. In contrast, Guan et al. (35) reported a decreased HSP60 immunoeexpression in the hypertrophied pancreatic islets cells of diabetic mice when compared to the control mates. These consistent observations might reflect the failure of the anti-aging adaptive response of the islet cells as formerly demonstrated by Gomez (9).

When correlating the heat shock response with the cellular infiltration observed in the H&E staining, the HSP60 expression was significantly increased in the high-dose group which might reflect a stress-resistant effect to combat aging-related changes as an initial compensatory mechanism. The authors' suggestion was supported by Gomez (9) who demonstrated the vital role of immune/inflammatory cells in the aging process. These cells mediate the inflammatory/oxidative mechanisms in the body affecting longevity and aging progress. As a regulatory mechanism, HSP has increased to maintain the balance between these pro/anti-inflammatory mediators to keep healthy which agreed with the pattern of HSP60 expression.

Mechanistic Target of Rapamycin (mTOR) is an evolutionarily conserved protein kinase being activated by

phosphorylation and acts as an essential negative regulator in autophagy machinery. *unc-51*-like autophagy activating kinase (ULK1) is a serine/threonine protein kinase that contributes vitally to autophagy initiation (14). ULK1 is directly regulated by Adenosine Monophosphate-activated Protein Kinase (AMPK) and indirectly controlled by mTOR signaling (36). In the present study, a strong negative correlation existed. The *ULK1* gene expression was significantly decreased in the two-dose BPA groups, meanwhile a significant elevation in *mTOR* gene expression was noticed in the three organs according to the RT-PCR findings. Therefore, the ULK1 suppression might be due to either activated mTOR (addressed herein) or due to possible AMPK inactivation (37), resulting in deficient autophagy. This assumption was supported by Tang et al. (16) who reported that HSP60 overexpression is associated with AMPK suppression and mTOR pathway activation leading the glioblastoma cell proliferation. Hence, the authors suggested HSP60-induced activation of mTOR signaling followed by autophagy inhibition. In contrast, Quan et al. (38) and Lin et al. (39) reported BPA-induced inhibition of the mTOR pathway and autophagy stimulation in the rat's testis and mouse ovary, respectively. This conflict may be due to the use of highly toxic dose of BPA, different animal strains, and or organ-specific effect may exist.

As a stress response, the HSP60 expression was increased in an attempt to combat BPA-induced cell stress by enhancing protein folding efficacy, and any incompetent cells with uncorrected (mis/unfolded) proteins undergo chaperone-mediated autophagy (CMA) (40). Therefore, BPA could result in the accumulation of the damaged proteins in CMA-incompetent cells that escaped HSP repair. HSPs have a major role in apoptosis. HSP10 and HSP60 are pro-apoptotic (41), whereas others are anti-apoptotic (42). In correlation with the apoptotic changes observed in the H&E findings, the increased HSP60 expression might enhance, in part, the apoptotic cell death of the ailing cells that fail to repair the damaged proteins, as a compensatory mechanism for defective autophagy. Our assumption was consistent with Tang et al. (41) who suggested a context-dependent enhancement of apoptosis by HSP60. This means a balanced heat shock response (stress resistance) that led to the instant repair of damaged proteins and apoptosis of the stressed cells (with unrepaired protein), hence attempting to expand the life span.

In conclusion, the current two-dose-BPA exposures exerted a state of oxidative stress, low-grade inflammation, enhancement of the heat shock response, upregulation of the *mTOR* signaling, and downregulation of the autophagy machinery indicated by *ULK1* gene suppression. Collectively, the authors suggested complementary mechanisms that may interact/and or overlap to modulate Klotho expression in the kidney, liver, and pancreas. HSP60 expression pattern might compensate for the induced cellular stress and might enhance mTOR signaling during the 45-day duration of the experiment. Further in-depth studies are warranted for confirmation of the direct link between BPA and cellular aging. The research could provide another tool for directing more governmental attention to minimize BPA environmental pollution and inspiring individuals to adopt a safer lifestyle attitude.

Acknowledgements

The authors extend their appreciation to the Researchers Supporting Project number (RSPD2023R759), King Saud University, Riyadh, Saudi Arabia.

Interest conflict

The authors have declared no conflict of interest.

Consent for publications

The author read and approved the final manuscript for publication.

Availability of data and material

All data generated during this study are included in this published article.

Authors' Contribution

All authors had equal roles in study design, work, statistical analysis and manuscript writing.

Funding

The Researchers Supporting Project number (RSPD2023R759), King Saud University, Riyadh, Saudi Arabia.

Ethics approval and consent to participate

The proposal of the study was granted ethical approval by the Institutional Review Board (IRB), College of Medicine, King Saud University, Saudi Arabia (IRB #: KSU-SE-20-37).

References

- Harrison SM, Monahan FJ, Cummins E, Brunton NP. Bisphenol A and Metabolites in Meat and Meat Products: Occurrence, Toxicity, and Recent Development in Analytical Methods. *Foods* 2021;10:714.
- Buchanan S, Combet E, Stenvinkel P, Shiels PG. Klotho, aging, and the failing kidney. *Front Endocrinol (Lausanne)* 2020;11:1–15.
- Rao Z, Zheng L, Huang H, Feng Y, Shi R. α -klotho expression in mouse tissues following acute exhaustive exercise. *Front Physiol* 2019;10:1498.
- Typiak M, Piwkowska A. Antiinflammatory actions of klotho: implications for therapy of diabetic nephropathy. *Int J Mol Sci* 2021;22:956.
- Cheikhi A, Barchowsky A, Sahu A, Shinde SN, Pius A, Clemens ZJ, et al. Klotho: an elephant in aging research. *Journals Gerontol Ser A* 2019;74:1031–42.
- Aman Y, Schmauck-Medina T, Hansen M, Morimoto RI, Simon AK, Bjedov I, et al. Autophagy in healthy aging and disease. *Nat Aging* 2021;1:634–50.
- Lin MG, Hurley JH. Structure and function of the ULK1 complex in autophagy. *Curr Opin Cell Biol* 2016;39:61–8.
- Mantej J, Polasik K, Piotrowska E, Tukaj S. Autoantibodies to heat shock proteins 60, 70, and 90 in patients with rheumatoid arthritis. *Cell Stress Chaperones* 2019;24:283–7.
- Gomez CR. Role of heat shock proteins in aging and chronic inflammatory diseases. *GeroScience* 2021;43:2515–32.
- Kishimoto S, Uno M, Nishida E. Molecular mechanisms regulating lifespan and environmental stress responses. *Inflamm Regen* 2018;38:1–7.
- Lang BJ, Guerrero ME, Prince TL, Okusha Y, Bonorino C, Calderwood SK. The functions and regulation of heat shock proteins;

- key orchestrators of proteostasis and the heat shock response. *Arch Toxicol* 2021;95:1943–70.
12. Huang Y-H, Wang F-S, Wang P-W, Lin H-Y, Luo S-D, Yang Y-L. Heat Shock Protein 60 Restricts Release of Mitochondrial dsRNA to Suppress Hepatic Inflammation and Ameliorate Non-Alcoholic Fatty Liver Disease in Mice. *Int J Mol Sci* 2022;23:577.
 13. Liu GY, Sabatini DM. mTOR at the nexus of nutrition, growth, ageing and disease. *Nat Rev Mol Cell Biol* 2020;21:183–203.
 14. Weichhart T. mTOR as regulator of lifespan, aging, and cellular senescence: a mini-review. *Gerontology* 2018;64:127–34.
 15. Papadopoli D, Boulay K, Kazak L, Pollak M, Mallette FA, Topisirovic I, et al. mTOR as a central regulator of lifespan and aging. *F1000Research* 2019;8.
 16. Tang H, Li J, Liu X, Wang G, Luo M, Deng H. Down-regulation of HSP60 suppresses the proliferation of glioblastoma cells via the ROS/AMPK/mTOR pathway. *Sci Rep* 2016;6:1–11.
 17. Moon MK, Jeong I-K, Jung Oh T, Ahn HY, Kim HH, Park YJ, et al. Long-term oral exposure to bisphenol A induces glucose intolerance and insulin resistance. *J Endocrinol* 2015;226:35–42.
 18. Mersal E, Morsi AA, Alakabawy S, Elfawal RG, Sakr EM, Abdelmoneim AM, et al. Quantitative determination of Phthalate esters and Bisphenol-A residues in wastewater treatment plants outflow in Saudi Arabia: gas chromatography/mass spectrometry-based analytical study. *Egypt J Chem* 2022. ;65(13):1353-1360.
 19. EFSA Panel on Food Contact Materials Flavourings and Processing Aids (CEF) E. Scientific opinion on the risks to public health related to the presence of bisphenol A (BPA) in foodstuffs. *EFSA J* 2015;13:3978.
 20. Grotto D, Maria LS, Valentini J, Paniz C, Schmitt G, Garcia SC, et al. Importance of the lipid peroxidation biomarkers and methodological aspects for malondialdehyde quantification. *Quim Nova* 2009;32:169–74.
 21. Sun YI, Oberley LW, Li Y. A simple method for clinical assay of superoxide dismutase. *Clin Chem* 1988;34:497–500.
 22. Montgomery HAC, Dymock JF. Nitric oxide assay. *Analyst* 1961;86:414.
 23. Bancroft JD, Lyton C. The Hematoxylin and Eosin. In: Suvarna SK, Bancroft JD, Lyton C, editors. *Bancroft's theory Pract. Histol. Tech.* 8th ed, Ed, 2018, p. 126–38.
 24. Kiernan JA. Immunohistochemistry. In: Kiernan J, editor. *Histol. Histochem. methods. Theory Pract.* 4th-th ed., Scion Publishing Ltd; 2015, p. 454–90.
 25. Faul F, Erdfelder E, Buchner A, Lang A-G. Statistical power analyses using G* Power 3.1: Tests for correlation and regression analyses. *Behav Res Methods* 2009;41:1149–60.
 26. Liguori I, Russo G, Curcio F, Bulli G, Aran L, Della-Morte D, et al. Oxidative stress, aging, and diseases. *Clin Interv Aging* 2018;13:757.
 27. Collins BC, Laakkonen EK, Lowe DA. Aging of the musculoskeletal system: How the loss of estrogen impacts muscle strength. *Bone* 2019;123:137–44.
 28. Alekhya Sita GJ, Gowthami M, Srikanth G, Krishna MM, Rama Sireesha K, Sajjarao M, et al. Protective role of luteolin against bisphenol A-induced renal toxicity through suppressing oxidative stress, inflammation, and upregulating Nrf2/ARE/HO-1 pathway. *IUBMB Life* 2019;71:1041–7.
 29. Dutta M, Paul G. Gallic acid protects rat liver mitochondria ex vivo from bisphenol A induced oxidative stress mediated damages. *Toxicol Reports* 2019;6:578–89.
 30. Kim DY, Lee M, Kim EJ. Involvement of Klotho, TNF- α and ADAMs in radiation-induced senescence of renal epithelial cells. *Mol Med Rep* 2021;23:1.
 31. Zou D, Wu W, He Y, Ma S, Gao J. The role of klotho in chronic kidney disease. *BMC Nephrol* 2018;19:1–12.
 32. Yan F, Feng Y, Chen J, Yan J. Klotho downregulation contributes to myocardial damage of cardiorenal syndrome in sepsis. *Mol Med Rep* 2020;22:1035–43.
 33. Kikis EA. The intrinsic and extrinsic factors that contribute to proteostasis decline and pathological protein misfolding. *Adv Protein Chem Struct Biol* 2019;118:145–61.
 34. Sun Z, Zheng W, Teng J, Fang Z, Lin C. Resveratrol Reduces Kidney Injury in a Rat Model of Uremia and is Associated with Increased Expression of Heat Shock Protein 70 (Hsp70). *Med Sci Monit* 2020;26:e919086–e919086. <https://doi.org/10.12659/MSM.919086>.
 35. Guan S-S, Sheu M-L, Yang R-S, Chan D-C, Wu C-T, Yang T-H, et al. The pathological role of advanced glycation end products-downregulated heat shock protein 60 in islet β -cell hypertrophy and dysfunction. *Oncotarget* 2016;7:23072–87. <https://doi.org/10.18632/oncotarget.8604>.
 36. Holczer M, Hajdú B, Lőrincz T, Szarka A, Bánhegyi G, Kapuy O. Fine-tuning of AMPK–ULK1–mTORC1 regulatory triangle is crucial for autophagy oscillation. *Sci Rep* 2020;10:1–12.
 37. Wu M, Cong Y, Wang K, Yu H, Zhang X, Ma M, et al. Bisphenol A impairs macrophages through inhibiting autophagy via AMPK/mTOR signaling pathway and inducing apoptosis. *Ecotoxicol Environ Saf* 2022;234:113395. <https://doi.org/https://doi.org/10.1016/j.ecoenv.2022.113395>.
 38. Quan C, Wang C, Duan P, Huang W, Chen W, Tang S, et al. Bisphenol a induces autophagy and apoptosis concurrently involving the Akt/mTOR pathway in testes of pubertal SD rats. *Environ Toxicol* 2017;32:1977–89.
 39. Lin M, Hua R, Ma J, Zhou Y, Li P, Xu X, et al. Bisphenol A promotes autophagy in ovarian granulosa cells by inducing AMPK/mTOR/ULK1 signalling pathway. *Environ Int* 2021;147:106298.
 40. Kaushik S, Cuervo AM. The coming of age of chaperone-mediated autophagy. *Nat Rev Mol Cell Biol* 2018;19:365–81.
 41. Tang Y, Yang Y, Luo J, Liu S, Zhan Y, Zang H, et al. Overexpression of HSP10 correlates with HSP60 and Mcl-1 levels and predicts poor prognosis in non-small cell lung cancer patients. *Cancer Biomarkers* 2021;30:85–94.
 42. Wang S, Li X, Chen M, Storey KB, Wang T. A potential antiapoptotic regulation: The interaction of heat shock protein 70 and apoptosis-inducing factor mitochondrial 1 during heat stress and aestivation in sea cucumber. *J Exp Zool Part A Ecol Integr Physiol* 2018;329:103–11.